Gas Processing Journal

Vol. 11, No. 2, 2023, pp. 1 - 10
http://gpj.ui.ac.ir

Research Paper

Modeling and Emission Analysis of a Wankel Internal Combustion Engine through EES Software

Pouria Zonouzi [1], Mahdi Nami Khalilehdeh [1], Arash Nourbakhshsadabad [1], Ata khajehnasiri [1*], Seyed Faramarz Ranjbar [1*]

[1] Department of Mechanical Engineering, Faculty of Mechanical Engineering University of Tabriz, Tabriz, Iran

Received: 2024-09-11 Revised: 2024-12-07 Accepted: 2025-02-05

Abstract: The objective here is to assess the thermodynamic and environmental performance of Wankel engines, a distinctive internal combustion engine (ICE), by applying rotary design advantages. Unlike traditional reciprocating engines, Wankel engines due to their lower combustion chamber temperatures and pressure ratios exhibit unique emission profiles. Thermodynamic modeling through EES software is applied to simulate this Wankel engine's operation and compare its performance with conventional four-stroke reciprocating engines. The innovations here are analyzing the combustion parameters impact, on the chamber temperature exceeding 1800 K, on reducing greenhouse gases like CO_2 and NO_2, and evaluating water or steam injection methods to balance NOx and CO emissions. The optimization strategies for emission reductions through hydrogen and biofuels are assessed here. These findings provide new insights into enhancing the efficiency and sustainability of Wankel engines, offering practical implications for the development of cleaner combustion technologies.

keywords: Internal Combustion Engine, Combustion, Thermodynamic Modelling, Wankel Engine.

Highlights

- Modeling Wankel engine through EES software by solving the thermodynamic and combustion equations
- Predicting emission by applying the Zeldovich mechanism through the thermodynamics' second law
- Validation of results vs. a reliable reference for methane oxidation
- Lower emissions due to lower pressure and temperature; emissions drop as RPM increases

1. Introduction

The objective of applying an internal combustion engine is to transform the chemical energy stored in fuel into usable mechanical shaft power. As the fuel undergoes oxidation within the engine, the energy is released, leading to the reciprocating motion of the piston, which serves as the primary mechanism for power generation in the engine. The piston continuously oscillates between the bottom and top dead centers. At the bottom dead center, the fluid volume is at its maximum, and the top opposite holds. Wankel engines are of two-spark ignited and compression classes. This classification is determined by the engine compression ratio. The spark-ignited classes typically feature a compression ratio within the 8-12 range, while the compression class has a ratio within the 12-24 range [1].

The primary component of the Wankel engine is a rounded enclosure, which functions as its main body, where, a triangular rotor is installed, surrounded by cavities on its sides, which are designed to enhance the motor's volume. The rotation axis of the rotor is off-center of the motor's body, for the fluid's cycloid motion. Elevating the pressure within a Wankel engine does not necessitate high-octane fuel consumption. Consequently, the pressure ratio can be increased to enhance thermal efficiency. Unlike four-stroke engines, the Wankel engine

* **Corresponding Author.**
Authors' Email Address: [1] P. Zonouzi (pouria.zonoui@fgkinv.com**), [1] M. Nami Khalilehdeh** (mahdi.nami@tabrizu.ac.ir) , **[1] A. Nourbakhshsadabad** (a_nourbakhsh@tabriz.ac.ir), **[1] A. khajehnasiri** (ata.khajehnasiri@gmail.com) , **[1] S. F. Ranjbar** (s.ranjbar@tabrizu.ac.ir)

http://dx.doi.org/10.22108/GPJ.2025.142751.1139

has fewer rotating components. This decrease in rotating components leads to lower inertia and enables the Wankel engine to operate at higher velocities. The operational cycle of a conventional Wankel engine is detailed in [2, and 3].

Despite these advantages, incomplete combustion and emission issues persist in Wankel engines, as identified in previous studies. Spreitzer et al. [4] analyzed the combustion inefficiencies due to flame quenching in cavity corners, while Shi et al. [5] highlighted emission limitations. The computational approaches, proposed by [6 and 7], provide insights into flow dynamics and chemical reactions within Wankel engines. A detailed, validated thermodynamic model that integrates advanced emission prediction mechanisms remains underexplored. Addressing these gaps is critical for improving Wankel engine performance, especially subject to environmental and regulatory requirements.

This field is advanced by developing a comprehensive model for Wankel internal combustion engines through EES software, based on and extending the available findings. Unlike [4], where flame propagation challenges in Wankel engines are of concern, or [5], where the basic emission estimations are addressed, the advanced thermodynamic modeling is integrated with a second-law analysis for a more detailed prediction of pollutant emissions in this study. The inclusion of the Zeldovich mechanism for NOx prediction is a new aspect, offering higher accuracy compared to the traditional emission model applied in [6], where generalized pressure and temperature effects are applied without focusing on detailed reaction mechanisms.

This study introduces the validation method through the GRImech3.0 mechanism for methane oxidation and provides robust and reliable predictions of combustion processes. In contrast with [7], where leveraging advanced computational methods is evident, does not incorporate such a comprehensive validation approach as the one in this study. By explicitly analyzing the influence of operational pressure ratio, working temperature, and RPM parameters on emissions, a critical gap in understanding engine optimization, an area less assessed in this field is abridged.

This proposed methodology enhances the understanding of Wankel engine performance and aligns with global sustainability objectives by addressing the need for efficient, low-emission internal combustion engines. These new contributions push the studies forward in developing more environment-friendly engine technologies.

At the NASA Research Center, researchers applied a zero-dimensional model of thermodynamic performance to a rotary engine. This model is based on a supercharged Wankel engine with a single rotor. The performance conditions defined for this model engine are pressure and speed matrix. There exists a sample map through which the engine predicts its efficiency depending on different factors. After discussing this map, the engine heat transfer, the effect of material on engine performance and output energy, inlet valve pressure fluctuations and combustion chamber reaction, and the volume of loss and friction of seals are checked one by one [9]. A single-zone thermodynamic model is developed in [8] to assess the performance characteristics of a two-stroke Wankel engine, where two different port timings are applied. These findings indicate that the late opening and early closing port geometry (small opening area) with high supercharge pressure is of higher performance at a low-speed range and that upon an increase in rotor speed, the open period of the port area becomes insufficient for gas exchange, which reduces the power.

The global transition towards sustainable energy systems has induced integrated processes that enhance energy efficiency and reduce environmental impacts. Advanced configurations in combining renewable energy sources, waste heat recovery, and innovative cycles are promising potentials [10, and 11]. For instance, diffusion-absorption refrigeration and organic Rankine cycles are applied to hydrogen liquefaction, reducing specific power consumption to as low as 4.32 kWh/kgLH_2, with exergy efficiencies of over 53% [12]. Cryogenic energy storage systems that consume liquid air or nitrogen recovery have gained momentum in managing fluctuating energy demands. Such systems achieve storage and round-trip efficiencies exceeding 62%, with their exergy efficiency reaching 43.85%, making them crucial for peak demand scenarios [13]. Similarly, liquid natural gas (LNG) production processes leveraging solar energy and DMR compression refrigeration cycles exhibit specific energy consumption as low as 0.2293 kWh/kgLNG, next to economic advantages like a payback period of just over two years [14]. These advances highlight the importance of innovative solutions for reducing energy intensity in industrial applications.

Equally important are the integrated systems designed for emission reduction. Dual-pressure Linde-Hampson liquefaction systems, accompanied by post-combustion CO_2 capture, can extract 9307 kmol/h of CO_2 from power plant emissions while consuming geothermal and solar energy as low-cost heat sources. These systems achieve multi-functional round-trip efficiencies of 36.75% and show their viability for carbon management [15]. The mixed refrigeration cycles combined with organic Rankine cycles and solar energy in hydrogen and LNG production systems yield exceptionally high product recovery rates, like 98% for hydrogen, with specific power consumption as low as 0.1975 kWh/kg for both products [16]. These sophisticated designs reduce

greenhouse gas emissions and optimize energy consumption. Such developments next to the emission analysis of Wankel internal combustion engines, provide compact and efficient energy conversion solutions. By applying the EES software for detailed modeling, these engines are analyzed to enhance performance and minimize negative environmental impacts.

The objective here is to model the performance of a Wankel internal combustion engine by applying EES software and validate the results vs. real-world data. The advanced thermodynamic and combustion equations are solved here to accurately simulate engine behavior, predicting pollutant emissions through the second-law formulation and the Zeldovich mechanism, and validating these predictions vs. the GRImech3.0 mechanism for methane oxidation. Here the correlations among operational parameters like pressure ratio, temperature, and RPM—and emissions, contributing to the development of efficient, low-emission internal combustion engines aligned with global sustainability objectives are assessed.

2. Methods

The relevant governing equations are solved to establish a computational code within the EES software platform.

2-1 Wankel Engine Governing Equations

This Engine is considered a control Volume and the initial governing thermodynamic equations consist of the continuity and energy conservation [17].

$$\frac{dm_{accumulated}}{dt} = \overset{0}{m}_{in} - \overset{0}{m}_{out} \quad (1)$$

$$d(m_c e_c) = dm_{sc}h_{sc} - dm_{ex}h_{ex} - p_c dV_c + dQ_c \quad (2)$$

In Eq. (2), $d(m_c e_c)$ is the internal energy changes, m_{sc} h_{sc} is the inlet stream enthalpy, dm_{ex} h_{ex} is the outlet stream enthalpy and $p_c dV_c$ is the engine output work. The rejected heat dQ_c by this engine is explained in [18].

By expanding energy and ideal gas equations, the pressure changes in the combustion chamber are calculated through Eq. (3) [19]:

$$\frac{dp_c}{dt} = \frac{p_c}{V_c}\left(\mu_{sc}a_{sc}\psi_{sc}\sqrt{2RT_{sc}}\frac{p_{sc}}{p_c}k_{sc} - \mu_{ex}a_{ex}\psi_{ex}\sqrt{2RT_{ex}}k_c - k_c\frac{dV_c}{dt} + \frac{R}{p_c}\frac{1}{c_v}\frac{dQ_c}{dt}\right) \quad (3)$$

where Ψ is the flow function and the parameters are calculated through Eqs. (4-6):

$$\frac{dp_c}{d\phi} = \frac{1}{6n}\frac{dp_c}{dt} \quad (4)$$

$$\overset{0}{m} = \rho_0 A\psi\sqrt{2RT_0} \quad (5)$$

$$\psi = \sqrt{\frac{k}{k-1}\left[\left(\frac{p}{p_0}\right)^{\frac{2}{k}} - \left(\frac{p}{p_0}\right)^{\frac{k-1}{k}}\right]} \quad (6)$$

Due to the assumption that during the process the flow is subsonic, the critical pressure ratio is calculated through Eq. (7):

$$\left(\frac{p}{p_0}\right)_{critical} = \left(\frac{2}{k+1}\right)^{\frac{k}{k+1}} \quad (7)$$

It is evident that in the case of supersonic flow, the port that fluid flows through will be choked, thus, the flow factor will be empirically determined through Eqs. (8, and 9) [20, and 21].

$$\mu_{sc} = 0.92 - 0.18\frac{a_{sc}}{A_{sc}} \quad (8)$$

$$\mu_{ex} = 0.97 - 0.34\frac{a_{ex}}{A_{ex}} \quad (9)$$

2-2 Combustion Governing Equations

The governing equation for modeling the combustion process for ICE is Atomic Species, consisting of the first and second laws of thermodynamics and combustion kinetic. Atomic species states that the volume of atomic species will remain constant during the combustion process, [22, and 23]:

$$\sum_{i=1}^{n} \nu_i' M_i \rightarrow \sum_{i=1}^{n} \nu_i'' M_i \quad (10)$$

where, ν is the stochiometric factor on either side of reactants or products and M is the the molar mass of the respective species. The symbol n is the number of involved species. The first and second thermodynamic law equations to control volume are expressed through Eqs. (11, and 12) [4 and 24]:

$$\sum_{inlet} n_i \bar{h}_i = \sum_{outlet} n_i \bar{h}_i \quad (11)$$

$$ln\, K_p = \frac{-\Delta G^o}{\bar{R}T} \quad (12)$$

In equation 12, K_p is the equilibrium constant of the reaction which can be calculated through Eq. (13). Symbol ΔG^o is the Gibbs function which can be calculated through Eq. (14) [22-25]:

$$K_p = \left[\prod_{i=1}^{n} X_i^{\nu_i'' - \nu_i'}\right]\left(\frac{P}{P_o}\right)^{\sum \nu_i'' - \nu_i'} \quad (13)$$

$$\Delta G^o = \sum_{i=1}^{n} (\nu_i'' - \nu_i')\overline{g_i^o} \quad (14)$$

For better modeling each control volume is considered as a Perfectly Stirred Reactor (PSR), Fig. (1), which is a zero dimension where the reaction occurs homogenously.

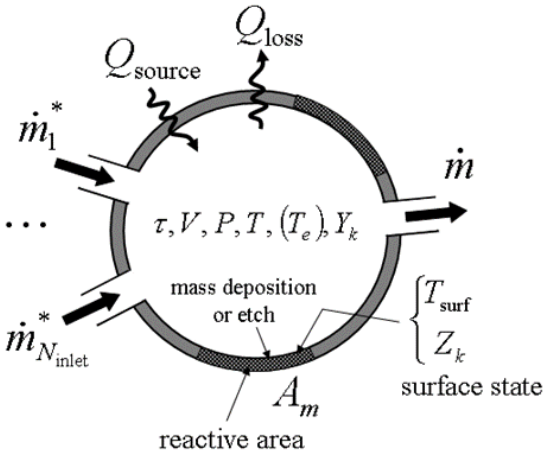

Fig. 1. Working Cycle of a Wankel Engine [1]

Continuity, atomic species and energy balance equations are expressed for a PSR as follows, respectively [1 and 26]:

$$\frac{d}{dt}(\rho V)_j = \sum_{i=1}^{N_{inlet}} \dot{m}_i^{*(j)} + \sum_{r=1}^{N_{PSR}} \dot{m}^{(r)} R_{rj} - \dot{m}^{(j)} + \sum_{m=1}^{M} A_m^{(j)} \sum_{k=1}^{K_g} \dot{S}_{k,m}^{(j)} W_k \quad (15)$$

where, ρ is the density, V is the volume of the PSR, and $\dot{m}$ is the mass flow rate of the inlet and m^* is the outlet mass flow rate; $S_{k,m}$ is the chemical species molar conversion rate of each species [1,27, and 28]:

$$(\rho V)^{(j)} \frac{dY_k^{(j)}}{dt} = \sum_{i=1}^{N_{inlet(j)}} \dot{m}^{*(j)} \left(Y_{k,i}^* - Y_k\right) + \sum_{r=1}^{N_{PSR}} \dot{m}^{(r)} R_{rj} \left(Y_k^{(r)} - Y_k^{(j)}\right) - Y_k^{(j)} \sum_{m=1}^{M} A_m^{(j)} \sum_{k=1}^{K_g} \dot{S}_{k,m}^{(j)} W_k + (\dot{\omega}_k V)^{(j)} W_k + \sum_{m=1}^{M} A_m^{(j)} \dot{S}_{k,m}^{(j)} W_k \quad (16)$$

where, W_k is the molecular weight, and Y_k is the mass fraction of each species.

2-3 Emission of pollutant species

The thermodynamic first and second law equations do not incorporate time, consequently, the time factor is not involved in these equations. To analyze the kinetics of this process its integral form should be solved. Through this approach, the volume of pollutant emission of the engine is calculated, while, first a proper mechanism for the production of these emitted species must be considered and the kinetic reaction should be solved. The emissions based on consumed fuel type by the engine are Nitrogen oxides, Sulfur Oxides, Unburned Hydrocarbons, and Volatile Organic Compounds. The Zeldovich mechanism is applied in Eq. (17) for the prediction of the reaction resulting in NO pollutant production [18].

$$\begin{aligned} O + N_2 &\rightleftarrows NO + N \\ N + O_2 &\rightleftarrows NO + O \\ N + OH &\rightleftarrows NO + H \end{aligned} \quad (17)$$

2.4 Input Data and Assumptions

The input data of the combustion chamber of the engine are tabulated in Table 3.

Table 1. Validation for Biomass Production Cycle

Parameter	This study	Experimental results [29]
Combustion chamber (bar) working pressure	3.9	3.88
Fuel mass flow rate (kg/s)	0.0712	0.0720
Flame adiabatic temperature (°K)	1800	1809
Combustion chamber length (mm)	120	119.7

Table 2. Validation for Air Flow rate

The mass flow rate of Air (Kg/s)	Quantity	Error (%)
GRI Mech 3.0	3.96	-
Experimental results [29]	3.97	-
This study	3.99	0.97%

In the Wankel engine model developed for this study applying EES software, boundary conditions, and thermodynamic properties are considered to simulate engine behavior in a range of operational conditions. In this study many key assumptions are made to simplify the modeling process, and introduce limitations that may influence the accuracy of the results, particularly at higher RPMs where flow dynamics vary significantly [30, and 31]:

Assumptions:

- **Subsonic Flow:** It is assumed that the flow within the combustion chamber remains subsonic throughout the engine's operation, which facilitates the simplification of the equations governing the flow dynamics. At higher RPMs, local flow velocities may reach or exceed the speed of sound, especially near the intake and exhaust ports, a phenomenon not addressed in this model, because it may introduce discrepancies in predicting flow dynamics and associated thermodynamic behavior at extreme operating conditions.
- **Perfectly Stirred Reactor (PSR):** The combustion chamber is modeled as a PSR, assuring a homogeneous mixing of reactants and products. This idealization ignores spatial and temporal gradients in temperature, pressure, and

species' concentration that are likely to occur in real-world engine operation, especially in high-speed conditions where mixing and combustion rates are not uniform.

- **Constant Thermodynamic Properties:** Some thermodynamic properties, like the heat capacity, specific volume, and enthalpy, remain constant over the range of operating conditions. This assumption significantly simplifies the calculations but may fail to capture the non-linear variations in these properties with temperature and pressure, particularly at high RPMs where sharp gradients in operating conditions occur.
- **Combustion Equilibrium:** The combustion process is assumed to achieve chemical equilibrium, based on Gibbs free energy minimization. This assumption disregards kinetic limitations that might arise at high-pressure and high-temperature conditions, where the reaction rates of key species may deviate from equilibrium. Such deviations can significantly affect the accuracy of emission predictions, particularly for pollutants like NOx.
- **Boundary Conditions for RPM Variations:** At higher RPMs, the intake and exhaust processes experience significant variations in flow velocity, pressure, and temperature. In this model, the boundary conditions are simplified, by assuming steady-state operation and neglecting transient effects like backflow or pressure waves in the intake and exhaust manifolds. These transient effects, common at high RPMs, could lead to discrepancies between the simulated and actual engine performance.

Though these assumptions contributive in providing a computationally efficient model, by introducing idealizations that may not fully represent the complexities of real-world Wankel engine operation. To address these restrictions, future studies should incorporate transient analysis, variable thermodynamic properties, and a more detailed treatment of flow dynamics, especially in high-RPM conditions. Validation vs. experimental data in different operational conditions will help identify and mitigate the discrepancies introduced by these assumptions.

3- Results

3-1 NO_x Estimation of Engine

The volume of NO_x Emission is studied through the developed code in this work. The results are tabulated in Table 3 and diagramed in Fig. (2).

Table 3. Results of NO_x estimation of engine

	Zeldovich	GRImech3.0	Error (%)
NO_x Emission (PPM)	29.25	29.20	0.17

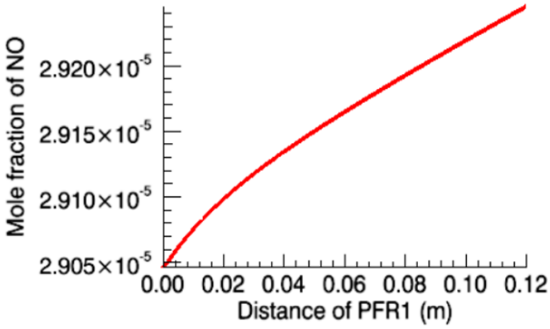

Fig. 2. The volume of NOx along the length of the combustion chamber

GRImech 3.0 predicts that at 1600°C the NO_x formation stops, while the Zeldovich mechanism predicts that NO_x Formation is still active at temperatures less than 1600°C, thus, the reason for the slight error in results.

3-2 Parametric Study

Combustion chamber temperature has a major impact on NO_x formation and an increase in temperature accelerates the NO_x formation and CO Emissions. Because the flame in a conventional combustion chamber typically exhibits diffusive characteristics, it is better to first assess the temperature variations of the flame within the combustion chamber, that is the inlet flow rate to the core reactor should be adjusted. The variations of temperature, NO mole fraction, CO mole fraction, and the volume of unburned hydrocarbons, as a function of the inlet air flow rate to the core reactor, respectively. The effect of process temperature is observed in Figs. (3 and 4a-b-c, and d) where the temperature variations, NO mole fraction, CO mole fraction, and the volume of unburned hydrocarbons, as a function of the inlet air flow rate to the region downstream of the flame, respectively.

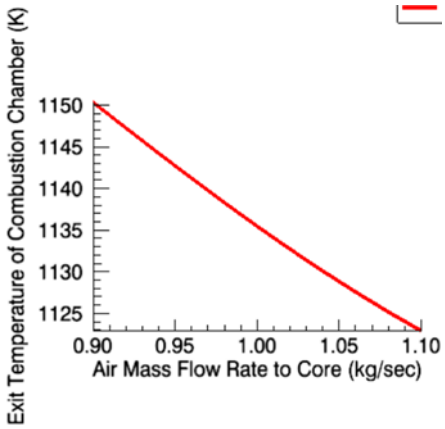

(3a)

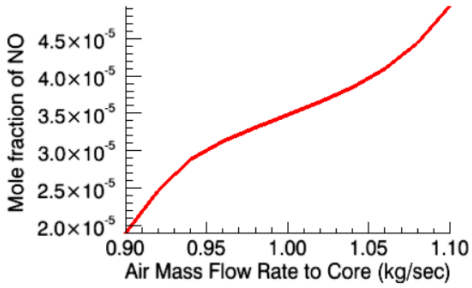

(3b)

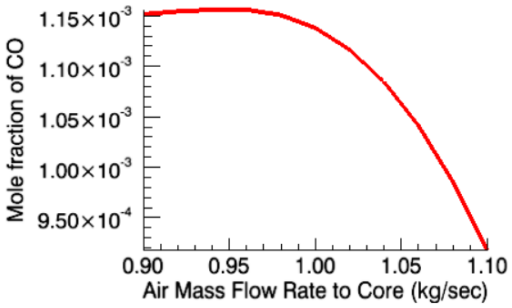

(3c)

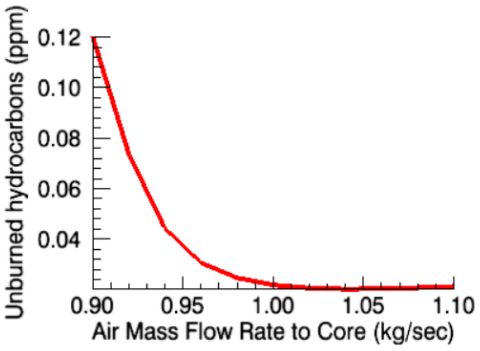

(3d)

Fig. 3: (3a) Output temperature profile of the combustion chamber vs. the inlet air flow rate to the core reactor. (3b) NO mole fraction profile vs. the inlet air flow rate to the core reactor. (3c) CO mole fraction profile vs. the inlet air flow rate to the core reactor. (3d) Unburned hydrocarbons profile vs. the inlet air flow rate to the core reactor.

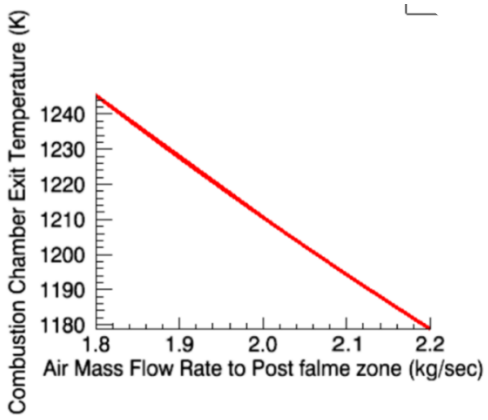

(a)

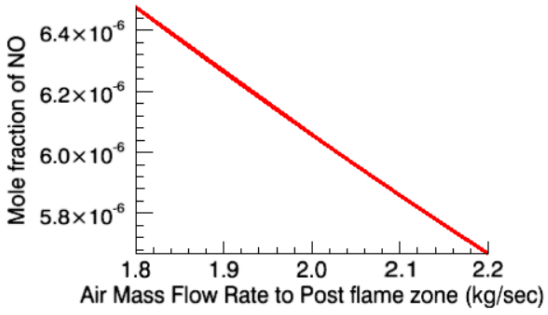

(b)

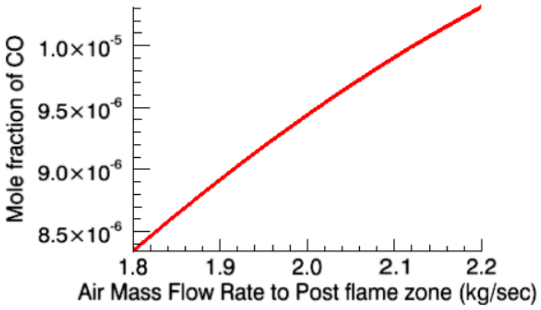

(c)

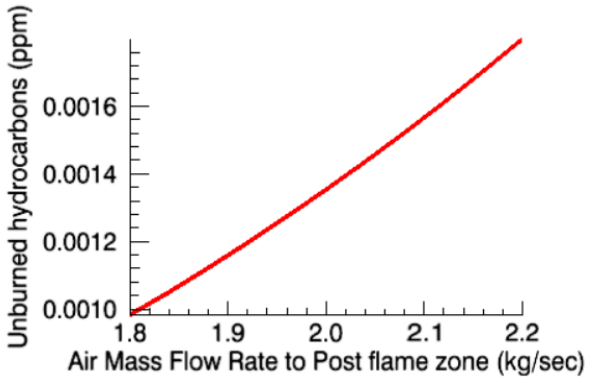

(d)

Fig. 4: (4a) Output temperature profile of the combustion chamber vs. the inlet air flow rate to the region downstream of the flame. (4b) NO mole fraction profile vs. the inlet air flow rate to the region downstream of the flame. (4c) CO mole fraction profile vs. the inlet air flow rate to the region downstream of the flame. (4d) Unburned hydrocarbons profile vs. the inlet air flow rate to the region downstream of the flame.

As observed in Fig. (4), an increase in the air intake mass flowrate decreases the temperature of the combustion process, thus, a decrease in total NOx Formation, while a decrease in the chamber drops the produced power of engine, Fig. (5).

This developed model is applied in modeling some of the real-produced engines like the two types of Mazda Wankel Engines, Fig. (6).

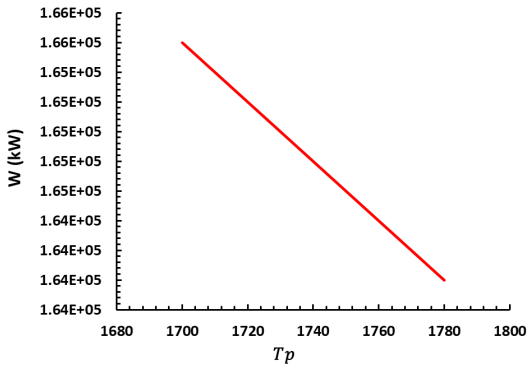

Fig. 5. The effect of exhaust temperature on power

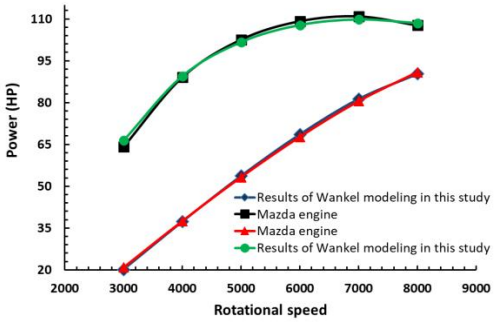

Fig. 6. The results of modeling two actual Wankel engines

The advancements in modeling NOx emissions in Wankel engines, by focusing on the accuracy of predictions using Zeldovich and GRImech 3.0 mechanisms are evident here, while the reliance of the available studies is on simplified models for NOx estimation. The slight differences among these mechanisms are valid when compared with the experimental data of Mazda Wankel engines. The inclusion of parametric studies on combustion chamber temperature and mass flow rates distinguishes this work by offering insights into optimizing both the emissions and power outputs. A comparison of the results obtained in this study with its counterparts is tabulated in Table 4.

Table 4- A comparison of the model's properties obtained in this study with those of other references [32, and 33]

Study	NOx Estimation Mechanisms	Key Findings on NOx Formation	Parametric Analysis	Validation Approaches	Novelty
This Study	Zeldovich, GRImech 3.0	NOx formation stops at 1600°C (GRImech 3.0); minor error (~0.17%).	Effect of temperature and air mass flow studied.	Validated with Mazda Wankel engine data.	Comprehensive comparison of NOx mechanisms; real-engine validation.
[32]	Simplified Zeldovich model	NOx formation is underpredicted at higher temperatures.	Temperature effect studied; no focus on airflow.	Simulation-based, no experimental validation.	Limited model; lacks accuracy for real-engine scenarios.
[33]	Computational Fluid Dynamics	NOx trends analyzed for diesel engines.	Effects of chamber design and fuels studied.	Validated for diesel engines, not rotary engines.	Focus on reciprocating engines; does not address rotary-specific issues.

4- Conclusion

The focus here is on modeling an internal combustion Wankel engine through the EES software. The governing equations of thermodynamics and combustion are applied to represent the engine's behavior accurately. To predict the emission of pollutants, the second law formulation is applied, next to the Zeldovich mechanism in this model. The obtained results are validated vs. the GRImech3.0 mechanism for methane oxidation, which demonstrates a satisfactory level of agreement. The Wankel engine exhibits a lower pressure ratio and working temperature compared to conventional reciprocating engines, thus, reducing emissions. An increase in the motor's RPM leads to a decrease in pollution levels because the reaction has almost no time to generate pollutants.

Future work could focus on expanding the emission modeling by incorporating additional chemical reaction mechanisms, like those considered for industrial soot and hydrocarbon formation. Assessing the consumption of hydrogen, syngas, or biofuels in the Wankel engine could provide valuable insights into its adaptability for cleaner energy applications in the gas processing industry. Optimization efforts would improve thermal efficiency through advanced materials or better cooling systems which would further enhance the engine's performance and emission control.

More studies regarding hybrid configurations

where the Wankel engine complements gas turbines or other machinery in gas processing systems will potentially increase the overall efficiency and emissions management. Conducting long-term real-world tests in operational gas processing plants would offer practical insights into the engine's reliability and commercial feasibility. Further refinement of the thermodynamic model by including advanced heat transfer and fluid dynamics would improve the accuracy of performance predictions under demanding conditions.

The key findings here are:

- **Enhanced NOx Prediction Accuracy:** The low error margin of 0.17% between Zeldovich and GRImech 3.0 models, obtained here is an improvement over typical values obtained in prior studies in this context
- **Parametric Analysis:** The findings demonstrate the dual impact of combustion chamber temperature on emissions and power, providing practical guidelines for engine optimization

4-1 Strengths and weaknesses

Significant innovations, like incorporating the Zeldovich mechanism for precise NOx emission predictions with its validation vs. the established methane oxidation datasets are introduced here. The comprehensive modeling approach provides a deeper understanding of the interdependence between operational parameters and emissions. The critical gaps in existing literature are addressed here and for its abridgment, a detailed thermodynamic analysis of Wankel engines is offered next to demonstrating the potential for optimizing their performance to meet contemporary environmental and efficiency standards.

While this study provides a comprehensive model for analyzing the performance and emissions of Wankel internal combustion engines, some limitations should not be overlooked. This modeling is limited to applying the Zeldovich mechanism and methane oxidation through the GRImech3.0 mechanism, where more complex chemical reactions like soot and hydrocarbon formation are not concerned. The influence of alternative fuels, which could further enhance the engine's environmental adaptability is not assessed here. The absence of long-term real-world testing, which would provide valuable insights into the engine's reliability, commercial feasibility, and adaptability under practical operating conditions is evident.

4-2 Suggestions for future works

To improve the accuracy of emission predictions, future works could consider integrating additional mechanisms to enhance the formation of hydrocarbons (HC) and carbon monoxide (CO). While the Zeldovich mechanism is effective for predicting NOx emissions, it may not be sufficient for HC and CO, particularly in varying engine operating conditions. The inclusion of more detailed mechanisms, like the extended Zeldovich mechanism for NOx, or models like the H2O2 and methane oxidation mechanisms (e.g., GRI-Mech 3.0) for hydrocarbons, could enhance predictions for unburned hydrocarbons (UHC) where the intermediate species in the combustion process are of concern. Adopting the Glarborg or Yuan model, and simulating the balance between CO formation and oxidation in the engine would improve CO emission predictions. Although integrating these models can increase computational complexities, they would provide a more accurate representation of emissions, thus, refining real-world applications and strategies for emission reduction in Wankel engines.

Nomenclature

h_{sc}	inlet stream enthalpy [Kj/Kg]
h_{ex}	outlet stream enthalpy [Kj/Kg]
Ψ	Fluid flow [m3 s-1]
v	stochiometric factor
M	the molar mass
ΔG^o	Gibbs function [Cal/K]
ρ	Density [m/s]
V	Volume [m^3]
$\dot{m}$	outlet mass flow rate [kg/s]
W_k	molecular weight [Kg/mol]

Reference

[1] P. Otchere, J. Pan, B. Fan, W. Chen, Y. Lu, Recent Studies of Fuels Used in Wankel Rotary Engines, J. Energy Resour. Technol. Trans. ASME. 143 (2021). https://doi.org/10.1115/1.4047971.

[2] J.B. Heywood, Internal combustion engine fundamentals / John B. Heywood., Intern. Combust. Engine Fundam. 2nd Ed. (2018).

[3] N. Watson, The thermodynamics and gas dynamics of internal combustion engines: Volume 1, Int. J. Heat Fluid Flow. 4 (1983). https://doi.org/10.1016/0142-727x(83)90012-7.

[4] J. Spreitzer, F. Zahradnik, B. Geringer, Implementation of a Rotary Engine (Wankel Engine) in a CFD Simulation Tool with Special Emphasis on Combustion and Flow Phenomena, in: SAE Tech. Pap., 2015. https://doi.org/10.4271/2015-01-0382.

[5] C. Shi, C. Ji, S. Wang, J. Yang, Z. Ma, P. Xu, Assessment of spark-energy allocation and ignition environment on lean combustion in a twin-plug Wankel engine, Energy Convers. Manag. 209 (2020). https://doi.org/10.1016/j.enconman.2020.112597.

[6] M.A. Patterson, S.C. Kong, G.J. Hampson, R.D. Reitz, Modeling the effects of fuel injection characteristics on diesel engine soot and NOx emissions, in: SAE Tech. Pap., 1994. https://doi.org/10.4271/940523.

[7] M.S. Rajut, E.A. Willis, Analysis of rotary engine combustion processes based on

unsteady, three-dimensional computations, in: 28th Aerosp. Sci. Meet. 1990, 1990. https://doi.org/10.2514/6.1990-643.

[8] O.A. Kutlar, F. Malkaz, Two-stroke Wankel type rotary engine: A new approach for higher power density, Energies. 12 (2019). https://doi.org/10.3390/en12214096.

[9] Y. Mito, K. Tanzawa, M. Watanabe, Y. Eiyama, Advanced combustion performance for high efficiency in new I3 1.2L supercharged gasoline engine by effective use of 3D engine simulation, in: SAE Tech. Pap., 2012. https://doi.org/10.4271/2012-01-0422.

[10]A. Ebrahimi, B. Ghorbani, M. Taghavi, Novel integrated structure consisting of CO2 capture cycle, heat pump unit, Kalina power, and ejector refrigeration systems for liquid CO2 storage using renewable energies, Energy Sci. Eng. 10 (2022). https://doi.org/10.1002/ese3.1211.

[11]A. Ebrahimi, B. Ghorbani, F. Skandarzadeh, M. Ziabasharhagh, Introducing a novel liquid air cryogenic energy storage system using phase change material, solar parabolic trough collectors, and Kalina power cycle (process integration, pinch, and exergy analyses), Energy Convers. Manag. 228 (2021) 113653. https://doi.org/10.1016/j.enconman.2020.113653.

[12]M. Taghavi, C.J. Lee, Development of novel hydrogen liquefaction structures based on waste heat recovery in diffusion-absorption refrigeration and power generation units, Energy Convers. Manag. 302 (2024). https://doi.org/10.1016/j.enconman.2023.118056.

[13]A. Ebrahimi, B. Ghorbani, M. Taghavi, Pinch and exergy evaluation of a liquid nitrogen cryogenic energy storage structure using air separation unit, liquefaction hybrid process, and Kalina power cycle, J. Clean. Prod. 305 (2021). https://doi.org/10.1016/j.jclepro.2021.127226.

[14]Z.A. Afrouzy, M. Taghavi, Thermo-economic analysis of a novel integrated structure for liquefied natural gas production using photovoltaic panels, J. Therm. Anal. Calorim. 145 (2021). https://doi.org/10.1007/s10973-021-10769-4.

[15]B. Ghorbani, G. Salehi, A. Ebrahimi, M. Taghavi, Energy, exergy and pinch analyses of a novel energy storage structure using post-combustion CO2 separation unit, dual pressure Linde-Hampson liquefaction system, two-stage organic Rankine cycle, and geothermal energy, Energy. 233 (2021). https://doi.org/10.1016/j.energy.2021.121051.

[16]A. Ahmadinejad, A. Ebrahimi, B. Ghorbani, Pinch and exergy assessment of an innovative hydrogen and methane purification process configuration based on solar renewable energy, Fuel. 359 (2024). https://doi.org/10.1016/j.fuel.2023.130391.

[17]M. Mabadi Rahimi, H., Jazayeri, S. A., Ebrahimi, Multi-Objective Optimization of a RCCI Engine Fueled with Diesel Fuel and Natural Gas Enriched with Hydrogen, Mabadi Rahimi, H., Jazayeri, S. A., Ebrahimi, M. 9 (2021) 33–42. https://doi.org/doi: 10.22108/gpj.2021.129302.1105.

[18]H.P. Berg, A. Himmelberg, T. Poojitganont, Hybrid Turbo Compound Fan Engine an Eco-Efficient Propulsion System for Aviation, in: IOP Conf. Ser. Mater. Sci. Eng., 2020. https://doi.org/10.1088/1757-899X/886/1/012010.

[19]B. Jafari, M. Seddiq, An Experimental Investigation of the Effects of Diesel Fuel Injection Characteristics in a Heavy-Duty Direct Injection (HDDI) Diesel Engine, Gas Process. J. 7 (2019) 53–64. https://doi.org/Jafari, B., Seddiq, M.

[20]S. Faramarzi, P. Esmat, E. Karimi, S. Abdollahi, Energy, exergy, economic, and sensitivity analyses of an enhanced liquid hydrogen production cycle within an innovative multi-generation system, J. Therm. Anal. Calorim. (2024). https://doi.org/https://doi.org/10.1007/s10973-024-12895-1.

[21]S. Faramarzi, S.M.M. Nainiyan, M. Mafi, R. Ghasemiasl, Energy, exergy, and economic analyses of an innovative hydrogen liquefaction process utilizing liquefied natural gas regasification system, Int. J. Exergy. 38 (2022) 442–456. https://doi.org/10.1504/ijex.2022.124614.

[22]S. Ghorbani, M. Khoshgoftar Manesh, Conventional and Advanced Exergetic and Exergoeconomic Analysis of an IRSOFC-GT-ORC Hybrid System, Gas Process. J. 8 (2020) 1–16. https://doi.org/doi: 10.22108/gpj.2019.119599.1067.

[23]S. Faramarzi, R. Ghasemiasl, F. Ghadami, Numerical investigation of the impact of inclined baffles and an elastic vibrating beam on the thermo-fluid behavior in a rectangular channel, SN Appl. Sci. 3 (2021). https://doi.org/10.1007/s42452-021-04568-7.

[24]S.E. Razavi, T. Adibi, S. Faramarzi, Impact of inclined and perforated baffles on the laminar thermo-flow behavior in rectangular channels, SN Appl. Sci. 2 (2020). https://doi.org/10.1007/s42452-020-2078-8.

[25]S. Faramarzi, S. Gharanli, M. Ramazanzade Mohammadi, A. Rahimtabar, A. J. Chamkha, Energy, exergy, and economic analysis of an innovative hydrogen liquefaction cycle integrated into an absorption refrigeration system and geothermal energy, Energy. 282 (2023) 128891. https://doi.org/10.1016/J.ENERGY.2023.128891.

[26]S. Faramarzi, S.M. Mousavi Nainiyan, M.

Mafi, R. Ghasemiasl, Genetic algorithm optimization of two natural gas liquefaction methods based on energy, exergy, and economy analyses: the case study of Shahid Rajaee power plant peak-shaving system, Gas Process. 9 (2021) 91–108. https://doi.org/10.22108/GPJ.2021.126527.1097.

[27]A. Nourbakhsh, M.N. Khalilehdeh, S. Faramarzi, M. Mafi, Energy, exergy and economic analysis of a hydrogen liquefaction process integrated with a PRICO cycle, Gas Process. J. 9 (2021) 83–102.

[28]A.N. Saadabad, M.N. Khalilehdeh, F. Ranjbar, S. Faramarzi, F. Firouzy, Simulation, analysis and optimization of a non-emission process producing power, hydrogen gas and liquid hydrogen using solar energy and PEM electrolysis, J. Mech. Eng. 02 (2022) 26–48.

[29]Z.M. Nikolaou, J.Y. Chen, N. Swaminathan, A 5-step reduced mechanism for combustion of CO/H2/H2O/CH4/CO2 mixtures with low hydrogen/methane and high H2O content, Combust. Flame. 160 (2013). https://doi.org/10.1016/j.combustflame.2012.09.010.

[30]A.D. Kraus, J.R. Welty, A. Aziz, Introduction to Thermal and Fluid Engineering, 2011. https://doi.org/10.1201/b12301.

[31]S.L. Dixon, C.A. Hall, Fluid Mechanics and Thermodynamics of Turbomachinery, 2010. https://doi.org/10.1016/C2009-0-20205-4.

[32]A.T. Doppalapudi, A.K. Azad, Advanced Numerical Analysis of In-Cylinder Combustion and NOx Formation Using Different Chamber Geometries, Fire. 7 (2024). https://doi.org/10.3390/fire7020035.

[33]A. Rao, R.K. Mehra, H. Duan, F. Ma, Comparative study of the NOx prediction model of HCNG engine, Int. J. Hydrogen Energy. 42 (2017). https://doi.org/10.1016/j.ijhydene.2017.07.107.